SDHD-related head and neck paragangliomas & their natural course

Heesterman, B.L.

Berdine L Heesterman, Lisa M H de Pont, Berit M Verbist, Andel G L van der Mey, Eleonora P M Corssmit, Frederik J Hes, Peter Paul G van Benthem and Jeroen C Jansen

Journal of Neurological Surgery Part B: Skull Base, 2017

4

Age and tumor volume predict growth of carotid and vagal body paragangliomas

Abstract

Background: Treatment for head and neck paragangliomas (HNGPL) can be more harmful than the disease. After diagnosis, an initial period of surveillance is often indicated, and surgery or radiotherapy is reserved for progressive disease. With the aim to optimize this "wait and scan" strategy, we studied growth and possible predictors.

Design: A retrospective cohort study was conducted.

Setting: This study was conducted at a tertiary referral center for patients with HNPGL.

Methods: Tumor volume was estimated for 184 SDHD-related carotid and vagal body paragangliomas using sequential MR imaging. Cox regression was used to study predictors of tumor growth.

Results: The estimated fraction of growing tumors ranged from 0.42 after 1 year of follow-up to 0.85 after 11 years. A median growth rate of 10.4 and 12.0 %/year was observed for carotid and vagal body tumors, respectively. Tumor location, initial volume, and age ($p < 0.05$) were included in our prediction model. The probability of growth decreased with increasing age and volume, indicating a decelerating growth pattern.

Conclusions: We created a prediction model (available online), enabling a more individualized "wait and scan" strategy. The favorable natural course of carotid and vagal body paragangliomas was confirmed; although with long follow-up growth will be observed in most cases.

Introduction

Head and neck paragangliomas (HNPGL) are neuroendocrine tumors that arise from paraganglionic tissue associated with the parasympathetic nervous system. The most common location is the carotid body, other locations include the vagal, jugular, tympanic, and aortic bodies. Paragangliomas are often hereditary, in the Netherlands mutations in subunit-D of the succinate dehydrogenase (SDH) gene are the most common [1–3]. Mutations in this gene are associated with the occurrence of multiple head and neck paragangliomas, occasional pheochromocytomas, and a very low frequency of malignant transformation [4, 5]. Surgical resection is the primary treatment of head and neck paragangliomas, but radiotherapy may also be used to gain local control of the disease. However, head and neck paragangliomas generally show a very favorable natural course, and surgery carries a high risk of cranial nerve impairment due to their location near neurovascular structures. Therefore, a "wait and scan" policy is often adopted [6–12]. With the introduction of presymptomatic testing for causative genes, an increasing number of small paragangliomas is detected. For these asymptomatic tumors with no recorded growth, observation may be the best management initially [13]. Surgical or radiation therapy must be considered if evident growth occurs or if the tumor causes debilitating symptoms. To optimize this treatment strategy and further improve counseling of patients and their families, knowledge of the likelihood of (rapid) progression is essential. The natural course of head and neck paragangliomas was addressed in five case series [6–9]. All concluded that many paragangliomas (30 - 65%) remain stable and if progression is observed, growth is very slow [6–9]. However, predictors remain to be determined. Also, we recently defined new cut-off points for growth in carotid (10%) and vagal (25%) body tumors enabling more accurate estimation of tumor progression [14]. On a cohort of 184 SDHD-related head and neck paragangliomas, we studied growth rate and prognostic factors for growth.

Methods

Subjects

The database of the Laboratory for Diagnostic Genome Analysis (LDGA) of the Leiden University Medical Center (LUMC) was used to identify carriers of an SDHD germline

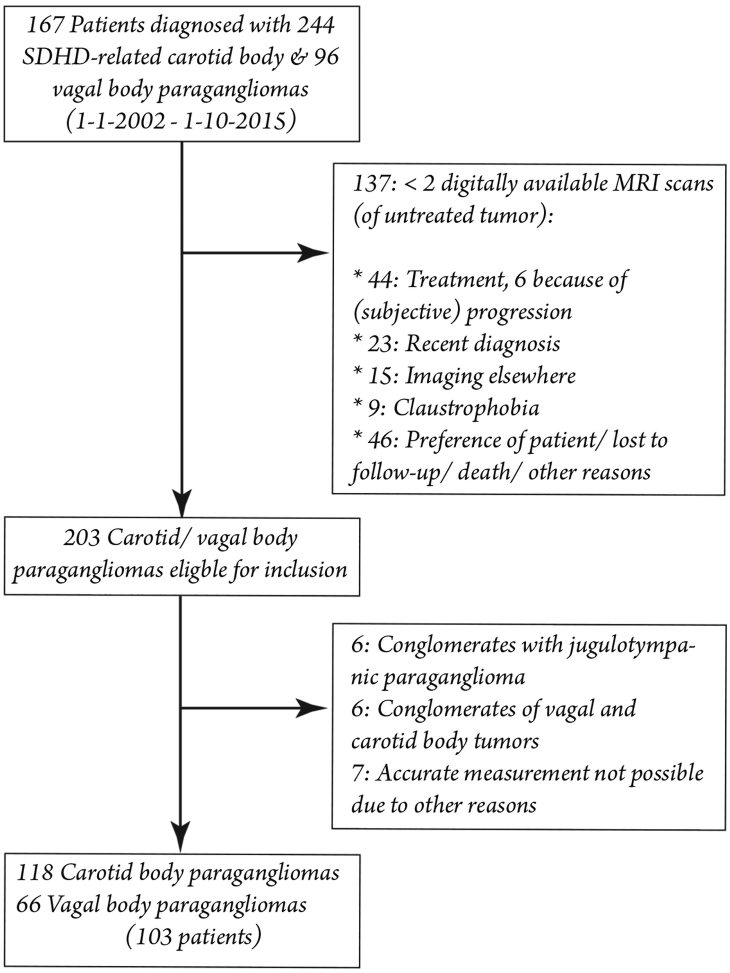

Figure 4.0.1: Carotid and vagal body paragangliomas included in this study

mutation. Subjects with a carrier status confirmed by molecular genetic testing as well as family members affected with paragangliomas (obligate carriers) were both eligible for inclusion if diagnosed with paragangliomas between January 2002 and October 2015. SDHD germline mutation carriers with the carotid body and/or vagal body paragangliomas managed with primary observation, and at least two digital available magnetic resonance imaging (MRI) scans of the head and neck region were selected. MRI scans are digitally available since 2002, to prevent selection bias, only subjects diagnosed since January 2002 were eligible for inclusion. Jugulotympanic tumors were not included as

we previously described that it was difficult to measure these tumors consistently [14]. Conglomerates of carotid and vagal body paragangliomas were measured as two separate tumors if possible, and otherwise excluded (figure 4.0.1). The date of the first digitally available MRI was considered the date of inclusion and time between the first and most recent digitally available MRI scan was considered the follow-up time. Relevant clinical parameters were retrieved from medical records.

According to the Dutch law, approval of the institutional ethics committee was not required, because all data used, were collected for routine patient care.

Volume estimation

At our institution, MRI is used as a diagnostic tool and for follow-up of patients with head and neck paragangliomas. Examinations were performed on 1.5T and 3T scans. Volume was estimated at the first ($T1$) and most recent ($T2$) digitally available MRI, on the contrast enhanced 3D Time of Flight (TOF) MR angiography sequence [14, 15]. Three perpendicular dimensions were used to calculate tumor volume, assuming an ellipsoid shape (figure 3.0.1 a & b).

$$Volume(V) = \frac{4}{3}\pi(\frac{1}{2}A * \frac{1}{2}B * \frac{1}{2}C) \tag{4.1}$$

All measurements were performed by two observers (BLH and LMHP). If measurements at the same time point differed more than the previously determined smallest detectable difference (10% for carotid body and 25% for vagal body parangliomas), consensus was reached [14]. Otherwise, the mean of both measurements was used for further calculations. Subsequently growth rate was calculated,

$$Growthrate(cm3/year) = \frac{V2 - V1}{T2 - T1} \tag{4.2}$$

$$Growthrate(\%/year) = \frac{1}{V1} * \frac{V2 - V1}{T2 - T1} \tag{4.3}$$

with $V1$ being the estimated volume at $T1$ and $V2$ the estimated volume at $T2$.

Statistics

The Statistical Package for Social Science (IBM SPSS Statistics, version 23.0, Armonk, New York, United States) and R version 3.2.5 were used for statistical analysis [16]. The Kaplan-Meier product limit estimator provided the estimated fraction of growing tumors and median time to growth. Cox proportional hazards regression with grouped jackknife variance estimator, to account for dependence amongst tumors from the same patient, was used to assess the relation between possible predictors and growth [17]. To differentiate growth from measurement error, growth was defined as a volume increase of at least 10% for carotid body and 25% for vagal body tumors [14]. If regression or progression less than the applicable cut-off value was observed, the censoring time was equal to follow-up time. If growth was observed, linear growth between $T1$ and $T2$ was assumed and time to growth (i.e., time to a volume increase of 10% or 25%) was calculated [18]. Age at inclusion, sex, mutation (p.Asp92Tyr versus other mutations in SDHD), initial volume ($V1$), tumor location (carotid versus vagal body paragangliomas) and whether a tumor was symptomatic or asymptomatic at its diagnosis, were considered possible predictors. Initial volume was positively skewed, and therefore $\log_2$ transformed, also natural cubic splines (df = 3) were used to relax the assumption of linearity. The proportional hazards assumption was checked, using scaled Schoenfeld residuals. To appraise the discriminative capability and predictive value, time-dependent receiver operating characteristic (ROC) curves (method: Nearest Neighbor Estimation, span 0.05) were produced and calibration plots (bootstrap cross-validated, with 100 cross-validation steps drawn with replacement, to prevent overfitting) were generated [19, 20]. To assess the relation between the development of new signs or symptoms and initial volume, volume increase and tumor location, a generalized estimation equation approach with robust estimator was used to account for within-patient correlation (exchangeable correlation matrix). Volume increase (cm^3) was positively skewed and for that reason categorized. Growth rate (%/year) of carotid and vagal body tumors, as well as, the initial volume of symptomatic and asymptomatic tumors were compared with a Mann-Whitney U Test. Statistical significance was considered for p-values <0.05. Continuous data are expressed as mean $\pm$ standard deviation if the data follows a normal distribution, if not, the median and interquartile range (IQR) are given unless stated otherwise.

Results

Subjects

A total of 184 paragangliomas, 118 carotid body and 66 vagal body tumors, diagnosed in 103 SDHD germline mutation carriers were included (figure 4.0.1). Overall, 64 (62%) subjects were males, and the median age at inclusion was 37 (range:13-62) years. The majority (80%) carried the c.274G>T, p.Asp92Tyr Dutch founder mutation, the remaining 21 subjects carried other previously described germline mutations in SDHD.

Growth characteristics

In a median follow-up time of 4.7 (IQR: 2.6-6.3) years, growth was observed in 75% of the carotid body (CBT) and 64% of vagal body paragangliomas (VBT). Regression was observed in 5%; the remaining tumors were stable. The median growth rate was 10.4 %/year for carotid body and 12.0%/year for vagal body tumors (p = 0.51). If only progressive tumors were considered, the median growth rate increased to 15.1% and 21.3% per year, for carotid and vagal body tumors, respectively, corresponding to a tumor doubling time of 5.9 and 4.7 years (table 4.0.1). The median time to growth was 1.4 (IQR: 0.5-5.1) years, and the estimated fraction of growing tumors was 0.42 (95% CI: 0.35-0.49) 1 year after inclusion and increased to 0.85 (95% CI: 0.70-0.92) after 11 years (figure 4.0.2).

Overall, 52 tumors were classified as clinically detected, with a lateral neck mass being the most reported symptom. Cranial nerve impairment attributable to tumor progression was observed in nine cases (4.9%), of which one developed during follow-up. The vagus nerve was affected most often. At the date of inclusion, 32% of the carotid body and 27% of vagal body tumors were symptomatic. The median volume of symptomatic tumors was substantially larger compared with asymptomatic tumors, 15.2 cm^3 (IQR: 6.4-24.3) versus 1.9 cm^3 (IQR: 0.7-4.9, p <0.001).

Clinical progression, defined as the progression of existing or development of new signs or symptoms, was reported in 66 cases (35.9%). In 45 cases new signs or symptoms were recorded, while in the remaining 21 cases it concerned progression of existing signs or symptoms. In most cases, it concerned the detection of a neck mass or progression of a

preexisting swelling. Other signs or symptoms, including medial bulging of the lateral pharynx wall, pain or discomfort, and dysphagia, were reported less often. There was a statistically significant relation between initial volume and the development of new signs or symptoms (odds ratio: 1.23, p = 0.04). With increasing volume expansion, new signs or symptoms were reported more often, although this relation was not statistically significant (odds ratio: 1.21 p = 0.07, appendix table 4.0.4). A total of 19 (10%) tumors (13 carotid and 6 vagal body tumors) were treated after *T2*. Conservative management was mainly (74%) discontinued because of evident progression. In the remaining cases, patients' preference was the most important reason for the switch to active treatment.

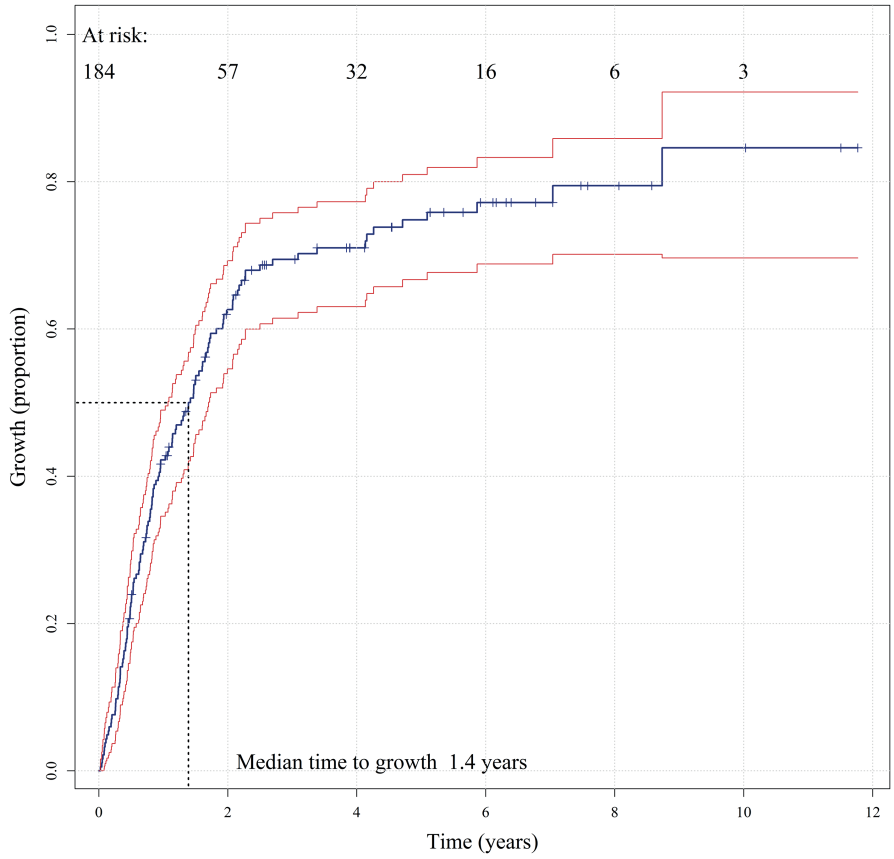

Figure 4.0.2: The cumulative proportion of growing tumors over time, with 95% confidence interval and numbers at risk.

Table 4.0.1: Growth characteristics and descriptives for carotid body tumors (CBT) and vagal body tumors (VBT)

	CBT		VBT	
	Median/N	IQR/%	Median/N	IQR/%
All	118		66	
Male	73	62 %	42	64 %
c.274G> T (p.Asp92Tyr)	89	75 %	52	79 %
Screening detected	82	69 %	50	76 %
Age (years)	37	30-50	40	30-51
Volume (cm^3)	3.0	0.9-9.3	3.8	1.2-16.8
Growth rate (cm^3/year)	0.26	0.05-0.76	0.41	0.08-1.46
Growth rate (%/year)	10.4	3.0-22.7	12.0	3.6-27.7
Growth	88	75 %	42	64 %
Male	55	62 %	27	64 %
c.274G> T (p.Asp92Tyr)	67	76 %	33	79 %
Screening detected	62	70 %	32	76 %
Age (years)	37	30-50	38	30-47
Volume (cm^3)	2.5	0.8-8.1	3.8	1.1-11.3
Growth rate (cm^3/year)	0.35	0.18-1.17	0.72	0.27-1.97
Growth rate (%/year)	15.1	6.8-30.0	21.3	12.3-35.3
T_d (years)	5.9	3.5-11.2	4.7	3.6-7.3
Stable	22	19 %	23	35 %
Regression	8	7 %	1	2 %

Predictors

At univariate and multivariate analysis tumor location, initial tumor volume (log_2 transformed) and age at inclusion were statistically significant predictors for growth, and were thus included in our prediction model (table 4.0.2). The hazard ratio of age was constant over time. This was however not true for carotid versus vagal body tumors. Therefore, tumor location was included in our prediction model as a stratification factor. Also, volume was nonproportional, but only for values between 0.03 cm^3 and 1.58 cm^3 (boundary to first internal knot), the associated parameter estimate was interpreted as an average effect [21].

Table 4.0.2: Multivariate Cox proportional hazards analysis predicting growth

	Hazard ratio (95% CI)	**p-value**
Age at inclusion [1]*	0.81 (0.69-0.95)	p = 0.01
Volume log_2 transformed *	0.86 (0.79-0.93)	p < 0.001
Location (ref = CBT) [2]*	0.63 (0.44-0.89)	p = 0.01
p.Asp92Tyr vs other SDHD variants (ref = other)	1.17 (0.72-1.91)	p = 0.53
Screening vs clinically detected (ref = screening detected)	1.34 (0.86-2.08)	p = 0.19
Sex (ref = male)	0.97 (0.65-1.46)	p = 0.88

[1] Hazard ratio for a 10-year increase in age
[2] Vagal body versus carotid body paragangliomas
* Included in our prediction model for growth

Prediction of growth

The predicted probability of growth decreased with increasing age and volume, increased over time and was higher for carotid body tumors compared with vagal body tumors (figure 4.0.3). For instance, if growth was predicted for a patient of 60 years with a carotid body tumor of 15 cm^3, the predicted probability of growth (volume increase to at least 16.5 cm^3) was 32% after 1 year of follow-up, 49% after 2 years, and increased to 60% after 5 years. In comparison, for a patient of 20 years with a carotid body tumor of 5 cm^3, the predicted probability of growth (volume increase to at least 5.5 cm^3) was 59%, 78% and 88%, respectively (appendix 4.0.6, an interactive version of the model is available at https://hnpgl.shinyapps.io/growth/).

Model performance

Median predicted probabilities were 35% (range 15 - 97%) for nongrowing tumors and 51% (range 17 - 92%) for growing tumors after the first year of follow-up, corresponding to an area under the curve (AUC) of 0.71. After 3 years of follow-up the median predicted probabilities were 72% (range: 41 - 100%) and 60% (range: 42 - 92%) for growing and nongrowing tumors, respectively (AUC: 0.64, figure 4.0.4a-b).

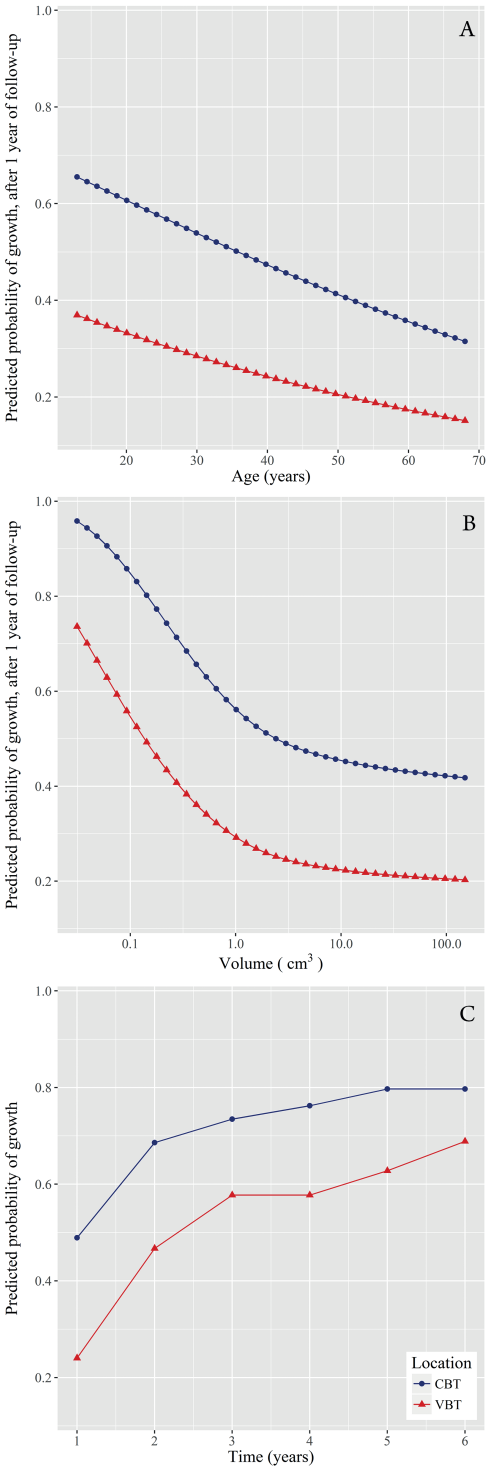

Figure 4.0.3: With increasing age and volume, the predicted probability of growth decreases. Figure 3a displays the relation between age (x-axis) and the predicted probability of growth after 1 year of follow-up (y-axis). The effect is illustrated for the median volume of carotid and vagal body paragangliomas (3.0 cm^3 and 3.8 cm^3). The relation between volume (x-axis) and predicted probability (y-axis) is illustrated in figure 3b, and displayed for a median age of 37 and 40 years for carotid and vagal body tumors, respectively. As shown in figure 3c, the predicted probability of growth increases over time (displayed for median values of age and volume).

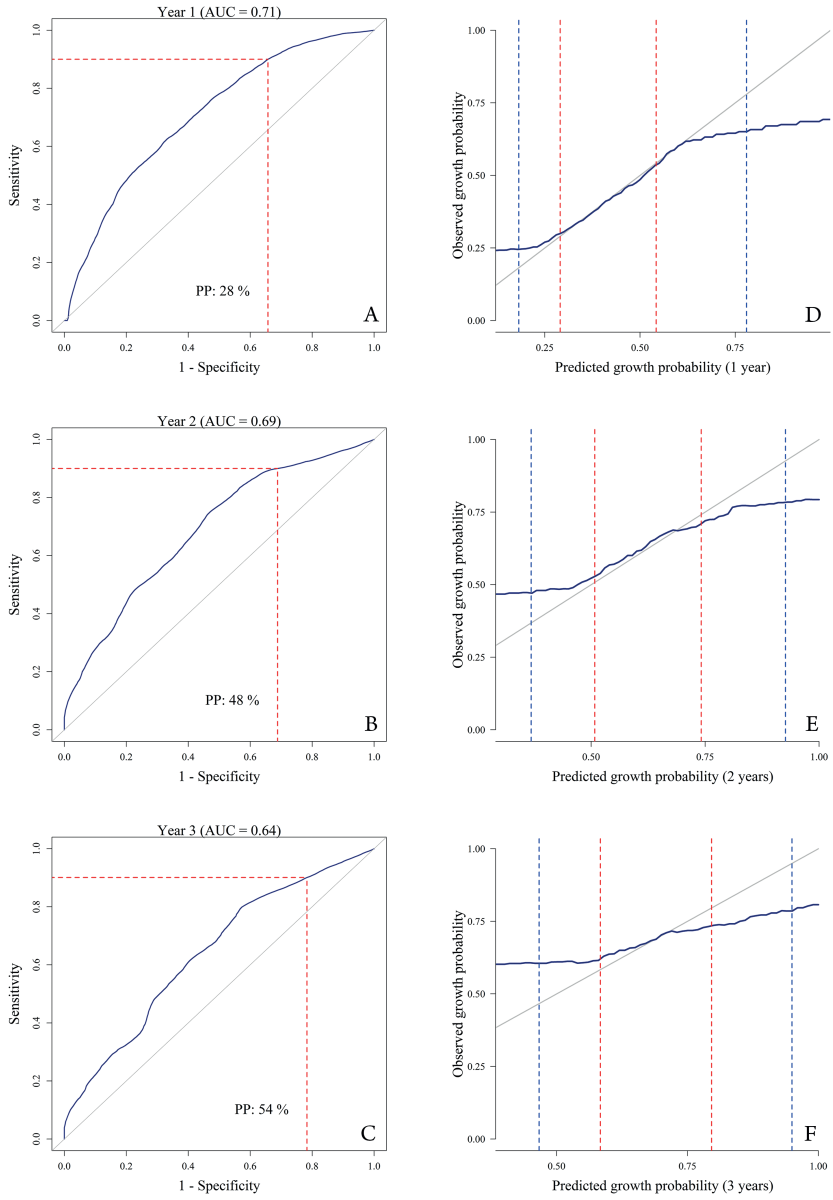

Figure 4.0.4: Time-dependent (after 1, 2, and 3 years of follow-up) ROC curves (figure 4 a-c) with the red lines indicating the 1- specificity and the predicted probability (PP) associated with a sensitivity of 90%. Figure 4 d-f: the corresponding calibration plots with the interquartile range (red lines) and 5th and 95th percentiles (blue dotted lines).

The observed and predicted growth probabilities were approximately equal for the interquartile range, the first 2 years of follow-up but diminished after that (figure 4.0.4 d-f).

Cut-offs for the predicted probability of growth

The consequences of using different cut-off values to make an MRI scan after 1 year of follow-up, with respect to scan reduction as well as number and characteristics of detected and missed growth are shown in table 4.0.3. A similar table with cut-offs for predicted probability after 2 years is provided in the appendix (table 4.0.5). If instead of screening all cases after 1 year, a scan would only be made if the predicted probability is equal to or higher than 34% (corresponding with a sensitivity of 80%), the number of scans would be reduced by 36%. By subsequently using 40% as cut-off value to make an MRI after 2 years (figure 4.0.5), the detection of growth would be delayed with 1 year in 19 cases (17%) and with 2 years in only one case (0.9%). Fast progression, defined as growth of more than 50% per year, was observed in a total of 19 cases and would be detected with 1-year delay in 3 (16%) cases (table 4.0.3 and appendix, table 4.0.6).

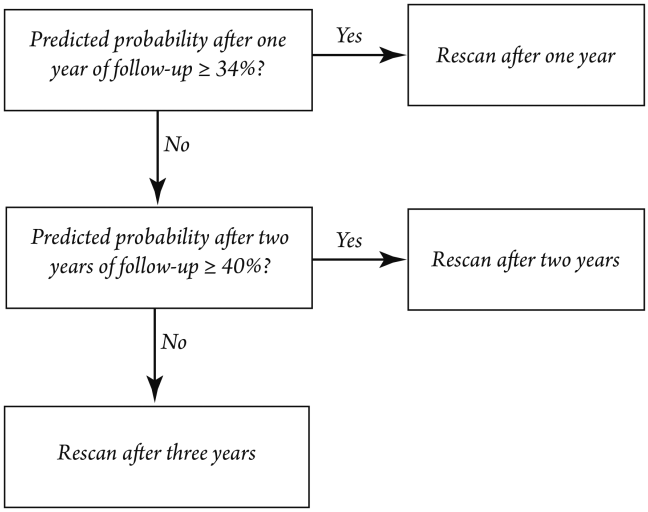

Figure 4.0.5: Screening strategy

Table 4.0.3: Number of detected and missed growth for several cut-offs of predicted probability

Cut-off value PP[1]	Sensitivity	No. of scans	Scan reduction (%)[2]	Detected growth	Missed growth (%)[3]	Detected fast progression [4]	Missed fast progression (%) [4,5]
18	99	171	8 (4)	76	1 (1)	19	0 (0)
24	95	150	29 (16)	73	4 (5)	17	2 (11)
28	90	138	41 (23)	70	7 (9)	16	3 (16)
32	85	125	54 (30)	65	12 (16)	16	3 (16)
34	80	115	64 (36)	62	15 (19)	16	3 (16)
37	75	106	73 (41)	59	18 (23)	15	4 (21)
40	70	93	86 (48)	53	24 (31)	15	4 (21)
42	65	86	93 (52)	51	26 (34)	14	5 (26)
46	60	75	104 (58)	47	30 (39)	13	6 (32)

[1] Cut-off values for predicted probability
[2] After 1 year 179 (97%) cases were still under follow-up
[3] % of total growth
[4] Fast progression is defined as progression > 50% /year
[5] % of total fast progression

Discussion

This study is the first to use multivariate Cox proportional hazards regression to examine the growth of head and neck paragangliomas, and thus factoring in varying follow-up time. We used tumor and measurement specific cut-off values for growth, resulting in a more robust estimation of tumor progression. A perhaps even more significant advantage of the model mentioned earlier is the possibility to study predictors. We found a statistically significant effect of volume, age, and tumor location on the probability of growth and created a prediction model for growth with fairly good discrimination and capability to correctly estimate the likelihood of growth.

With long follow-up growth is observed in most carotid and vagal body tumors, with the estimated fraction of growing tumors ranging from 42% after 1 year of follow-up to 85% after 11 years. However, with a median growth rate of 10.4% and 12.0% per year for carotid and vagal body tumors, respectively, progression is slow, especially in comparison with malignant tumors. In untreated glioblastoma, for instance, a median growth rate of 1.4% per day was observed [22]. Furthermore, cranial nerve impairment was reported in only one case, underlining the indolent natural course and safety of a "wait and scan" strategy. Carotid body tumors are measured more consistently compared with vagal body tumors, resulting in a smaller cut-off value for growth [14]. Consequently, the growth of carotid body tumors was observed earlier during follow-up, despite the higher growth rate of vagal body tumors.

Two earlier studies have addressed the growth of carotid and vagal body tumors; both also concluded that rapid progression is rare [6, 7]. Langerman and colleagues reported tumor growth in only 17 of 47 (38%) paragangliomas, during a mean follow-up time of 5 years. This relatively small percentage, compared with our results, may be partially explained by the comparatively high mean age of 56 (range: 17-86) years. Furthermore, it should be noted that three dimensions were available in only a limited number of cases and it was not clear how they differentiated between progressive and stable tumors. The current results are in agreement with our prior study, with the variation primarily the result of a different definition of growth (20% versus 10% and 25%). Also, the accuracy of measurements has increased as result of improved imaging techniques and digital available images (in our previous study all measurements were performed on hard copies).

Jugulotympanic tumors were not included in our present study. However, the growth of these tumors (Fish C1 to D1) was investigated by Carlson and colleagues [8]. They reported growth, defined as a volume increase of more than 20%, in 42% of tumors during a median follow-up time of 4.8 years. The relatively high median age of 70 years, may again partially explain the lower proportion of growing tumors. Also, the fact that the petrous bone largely surrounds these tumors may have influenced growth rate as well.

The decreasing probability of growth with both increasing volume and patients age, strongly indicate that paragangliomas exhibit a decelerating growth pattern. Both Gompertz and logistic models have been used to successfully model growth of tumors, predominantly in vitro [23]. Tumor doubling time was first introduced by Collins and colleagues to quantify growth rate and is based on exponential growth [24]. Although this model presumably describes early tumor growth, we anticipate that in the long run, a decelerating growth pattern is more accurate. The calculated median tumor doubling, of 5.9 and 4.7 years for carotid and vagal body tumors, is therefore likely to be an underestimation of true doubling time [23].

Currently, MR imaging of the head and neck is, at our institution, generally performed at intervals of 1 to 2 years. Our prediction model enables a more individualized approach. In addition to the predictive value of volume, age, and tumor location, these predictors largely determine treatment possibilities and outcome, as well as, the decision to switch from watchful waiting to active treatment if tumor growth is observed. Surgery for small carotid body tumors is relatively safe. However, the risk of cranial nerve impairment increases with tumor size and is particularly high (12.5% - 78.6%) if the tumor surrounds the carotid vessels. Other complications include permanent stroke and hemorrhage, and are more likely to occur if vascular repair is required [25, 26]. Therefore, surgery should be considered if growth is observed in a carotid body tumor, which may still be treated with low risk for complications. In comparison, surgery for vagal body tumors almost inevitably results in functional loss of the vagus nerve. Therefore, surgery is only advisable if tumor progression already resulted in lower cranial nerve impairment, if excessive catecholamine secretion is accompanied by symptoms or in the case of malignant disease (i.e., the presence of nodal or distant metastasis). Radiation therapy may also be used to gain local control. However, the risk of late complications, for instance, radiation-induced malignancy and carotid stenosis, should be weighed against the natural course [26,

27]. Considering the implications of tumor progression and the likelihood of changing to active treatment if growth is observed, our prediction model can be used to individualize screening intervals and thereby reduce the number of "unnecessary" scans.

It should be noted that although bootstrap cross-validation was used to prevent overfitting, the model is not (yet) externally validated. Also, the results presented here may not be applicable to sporadic cases. Even though a statistically significant difference between growth of hereditary and sporadic cases has previously not been observed, a comparatively lower growth rate is, considering sporadic HNPGL are on average diagnosed approximately 15 years later compared with hereditary cases, plausible [6, 8, 28]. Furthermore, the retrospective nature of this study, as well as the multifocality associated with mutations in the SDHD gene, preclude definitive conclusions regarding clinical progression.

Conclusion

This study, confirms the indolent growth of carotid and vagal body paragangliomas. We also established the predictive value of tumor location, volume, and patients' age. With increasing age and volume the probability of growth decreases, indicating a decelerating growth pattern. The use of these predictors in a model for growth facilitates a more individualized approach to "watchful waiting".

References

1. B. E. Baysal, R. E. Ferrell, J. E. Willett-Brozick, et al. "Mutations in SDHD, a mitochondrial complex II gene, in hereditary paraganglioma." In: *Science* 287.5454 (2000), pp. 848–851.
2. H. P. H. Neumann, Z. Erlic, C. C. Boedeker, et al. "Clinical predictors for germline mutations in Head and neck paraganglioma patients: cost reduction strategy in Genetic diagnostic process as fail-out". In: *Cancer Res.* 69.8 (2009), pp. 3650–3656.
3. R. F. Badenhop, J. C. Jansen, P. A. Fagan, et al. "The prevalence of SDHB, SDHC, and SDHD mutations in patients with head and neck paraganglioma and association of mutations with clinical features." In: *J. Med. Genet.* 41.7 (2004), e99.
4. D. E. Benn, B. G. Robinson, and R. J. Clifton-Bligh. "15 Years of paraganglioma: Clinical manifestations of paraganglioma syndromes types 1-5." In: *Endocr. Relat. Cancer* 22.4 (2015), T91–103.
5. L. T. van Hulsteijn, O. M. Dekkers, F. J. Hes, J. W. A. Smit, and E. P. M. Corssmit. "Risk of malignant paraganglioma in SDHB-mutation and SDHD-mutation carriers: a systematic review and meta-analysis". In: *J. Med. Genet.* (2012), pp. 768–776.
6. J. C. Jansen, R. van den Berg, A. Kuiper, A. G. van der Mey, A. H. Zwinderman, and C. J. Cornelisse. "Estimation of growth rate in patients with head and neck paragangliomas influences the treatment proposal." In: *Cancer* 88.12 (2000), pp. 2811–2816.
7. A. Langerman, S. M. Athavale, S. V. Rangarajan, R. J. Sinard, and J. L. Netterville. "Natural History of Cervical Paragangliomas: Outcomes of Observation of 43 Patients". In: *Arch. Otolaryngol. - Head Neck Surg.* 138.4 (2012), pp. 341–345.
8. M. L. Carlson, A. D. Sweeney, G. B. Wanna, J. L. Netterville, and D. S. Haynes. "Natural History of Glomus Jugulare: A Review of 16 Tumors Managed with Primary Observation". In: *Otolaryngol. – Head Neck Surg.* 152.1 (2014), pp. 98–105.
9. S. C. Prasad, H. A. Mimoune, F. D'Orazio, et al. "The role of wait-and-scan and the efficacy of radiotherapy in the treatment of temporal bone paragangliomas." In: *Otol. Neurotol.* 35.5 (2014), pp. 922–31.
10. J. C. Sniezek, J. L. Netterville, and A. N. Sabri. "Vagal paragangliomas". In: *Otolaryngol. Clin. North Am.* 34.5 (2001), pp. 925–939.
11. M. G. Moore, J. L. Netterville, W. M. Mendenhall, B. Isaacson, and B. Nussenbaum. "Head and Neck Paragangliomas: An Update on Evaluation and Management." In: *Otolaryngol. – Head Neck Surg.* 154.4 (2016), pp. 597–605.
12. P. Gilbo, C. G. Morris, R. J. Amdur, et al. "Radiotherapy for benign head and neck paragangliomas: A 45-year experience". In: *Cancer* 120.23 (2014), pp. 3738–3743.
13. B. L. Heesterman, J. P. Bayley, C. M. Tops, et al. "High prevalence of occult paragangliomas in asymptomatic carriers of SDHD and SDHB gene mutations." In: *Eur. J. Hum. Genet.* 21.4 (2013), pp. 469–70.
14. B. L. Heesterman, B. M. Verbist, A. G. L. van der Mey, et al. "Measurement of head and neck paragangliomas: is volumetric analysis worth the effort? A method comparison study." In: *Clin. Otolaryngol.* 41.5 (2016), pp. 571–8.

15. R. van den Berg. "Imaging and management of head and neck paragangliomas". In: *Eur. Radiol.* 15.7 (2005), pp. 1310–1318.
16. R. C. Team. *R: A Language and Environment for Statistical Computing*. Vienna, Austria, 2016.
17. T. M. Therneau. *A Package for Survival Analysis in S*. 2015.
18. J. T.-Y. Wang, A. Y.-Y. Wang, S. Cheng, L. Gomes, and M. Da Cruz. "Growth Rate Analysis of an Untreated Glomus Vagale on MRI". In: *Case Rep. Otolaryngol.* 2016 (2016), pp. 1–6.
19. U. B. Mogensen, H. Ishwaran, and T. A. Gerds. "Evaluating Random Forests for Survival Analysis using Prediction Error Curves." In: *J. Stat. Softw.* 50.11 (2012), pp. 1–23.
20. P. J. Heagerty and P. Saha-Chaudhuri. *survivalROC: Time-dependent ROC curve estimation from censored survival data*. 2013.
21. P. D. Allison. "Survival Analysis". In: *Rev. Guid. to Quant. Methods Soc. Sci.* Routledge, 2010, pp. 413–424.
22. A. L. Stensjøen, O. Solheim, K. A. Kvistad, A. K. Håberg, Ø. Salvesen, and E. M. Berntsen. "Growth dynamics of untreated glioblastomas in vivo". In: *Neuro. Oncol.* 17.10 (2015), pp. 1402–1411.
23. A. Talkington and R. Durrett. "Estimating Tumor Growth Rates In Vivo." In: *Bull. Math. Biol.* 77.10 (2015), pp. 1934–54.
24. V. P. Collins, R. K. Loeffler, and H. Tivey. "Observations on growth rates of human tumors." In: *Am. J. Roentgenol. Radium Ther. Nucl. Med.* 76.5 (1956), pp. 988–1000.
25. K. E. van der Bogt, M.-P. F. M. Vrancken Peeters, J. M. van Baalen, and J. F. Hamming. "Resection of carotid body tumors: results of an evolving surgical technique." In: *Ann. Surg.* 247.5 (2008), pp. 877–884.
26. C. Suárez, J. P. Rodrigo, W. M. Mendenhall, et al. "Carotid body paragangliomas: a systematic study on management with surgery and radiotherapy." In: *Eur. Arch. Otorhinolaryngol.* 271.1 (2014), pp. 23–34.
27. C. Suárez, J. P. Rodrigo, C. C. Bödeker, et al. "Jugular and vagal paragangliomas: Systematic study of management with surgery and radiotherapy." In: *Head Neck* 35.8 (2013), pp. 1195–204.
28. N. Burnichon, V. Rohmer, L. Amar, et al. "The succinate dehydrogenase genetic testing in a large prospective series of patients with paragangliomas." In: *J. Clin. Endocrinol. Metab.* 94.8 (2009), pp. 2817–2827.

Appendix

Table 4.0.4: Generalized estimation equation predicting the development of additional signs

	Odds ratio (95% CI)	p-value
Volume increase [1]	1.21 (0.98; 1.49)	p = 0.07
Initial volume [2]	1.23 (1.01; 1.50)	p = 0.04
Location (ref = CBT)	0.93 (0.49; 1.76)	p = 0.82

[1] Volume increase was categorized into 8 groups based on quantiles
[2] Initial volume (cm^3) was log2 transformed

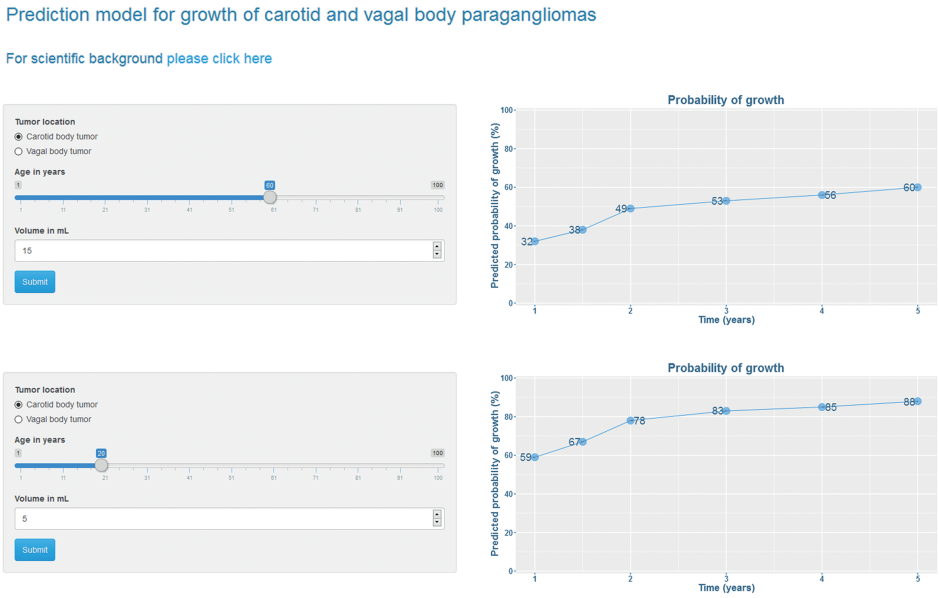

Figure 4.0.6: Prediction of growth for two fictitious patients, interactive version of model is available at https://hnpgl.shinyapps.io/growth/

Table 4.0.5: Number of detected and missed growth for several cut-offs of predicted probability, after 2 years of follow-up (assuming that no scans are made after 1 year of follow-up)

Cut-off value PP[1]	Sensitivity	No. of scans	Scan reduction (%)[2]	Detected growth	Missed growth (%)[3]	Detected fast progression [4]	Missed fast progression (%) [4,5]
33	99	165	2 (1)	109	1 (1)	19	0 (0)
40	95	154	13 (8)	104	6 (5)	19	0 (0)
48	90	140	27 (16)	100	10 (9)	17	2 (11)
51	85	125	42 (25)	93	17 (15)	17	2 (11)
53	80	116	51 (31)	88	22 (20)	16	3 (16)
55	75	108	59 (35)	83	27 (25)	16	3 (16)
57	70	100	67 (40)	78	32 (29)	16	3 (16)
59	65	91	76 (46)	71	39 (35)	16	3 (16)
61	60	87	80 (48)	69	41 (37)	16	3 (16)

[1] Cut-off values for predicted probability
[2] After 2 years 167 (91%) cases were still under follow-up
[3] % of total growth
[4] Fast progression is defined as progression > 50% /year
[5] % of total fast progression

Table 4.0.6: Number of detected and missed growth for several cut-offs of predicted probability after 2 years of follow-up, for cases that would not have been scanned after 1 year based on the screening strategy illustrated in figure 4.0.5. If subsequently 40% would be used as cut-off value to make an MRI after 2 years (screening algorithm illustrated in figure 4.0.5), growth would be missed in 6 additional cases. However, only in 1 out of these 6 cases growth could already have been detected after 1 year of follow-up. Therefore, the detection of growth would be delayed with 1 year in 19 cases (17%) and with 2 years in 1 case (0.9%). Furthermore, growth not yet detectable after 1 year of follow-up would be observed in 9 cases.

Cut-off value PP[1]	Sensitivity	No. of scans	Scan reduction (%)[2]	Detected growth (one year delay)	Missed growth (two years delay)	Detected fast progression [3]	Missed fast progression (%) [3,4]
33	99	58	2 (3)	28 (15)	1 (0)	3	0 (0)
40	95	47	13 (22)	23 (14)	6 (1)	3	0 (0)
48	90	33	27 (45)	19 (11)	10 (4)	1	2 (67)
51	85	18	42 (70)	12 (7)	17 (8)	1	2 (67)
53	80	13	47 (78)	8 (5)	21 (10)	0	3 (100)

[1] Cut-off values for predicted probability
[2] 93% of the cases with a predicted probability of less then 34% at year 1 were still under follow-up after 2 years. In the remaining 4 cases growth was not detected during follow-up
[3] Fast progression is defined as progression > 50% /year
[4] % of total fast progression